Available online at www.sciencedirect.com
SCIENCE DIRECT®
Journal of Computational Physics 197 (2004) 686–710
JOURNAL OF COMPUTATIONAL PHYSICS
www.elsevier.com/locate/jcp

Fully conservative finite difference scheme in cylindrical coordinates for incompressible flow simulations

Youhei Morinishi [a,*], Oleg V. Vasilyev [b], Takeshi Ogi [a]

[a] *Graduate School of Engineering, Nagoya Institute of Technology, Gokiso-cho, Showa-ku, Nagoya, Aichi 466-8555, Japan*
[b] *Department of Mechanical Engineering, University of Colorado, 427 UCB, Boulder, CO 80309, USA*

Received 8 September 2003; accepted 18 December 2003
Available online 24 January 2004

Abstract

A new finite difference scheme on a non-uniform staggered grid in cylindrical coordinates is proposed for incompressible flow. The scheme conserves both momentum and kinetic energy for inviscid flow with the exception of the time marching error, provided that the discrete continuity equation is satisfied. A novel pole treatment is also introduced, where a discrete radial momentum equation with the fully conservative convection scheme is introduced at the pole. The pole singularity is removed properly using analytical and numerical techniques. The kinetic energy conservation property is tested for the inviscid concentric annular flow for the proposed and existing staggered finite difference schemes in cylindrical coordinates. The pole treatment is verified for inviscid pipe flow. Mixed second and high order finite difference scheme is also proposed and the effect of the order of accuracy is demonstrated for the large eddy simulation of turbulent pipe flow.

Keywords: DNS; LES; Conservation properties; Finite difference scheme; Cylindrical coordinate; Staggered grid; Non-uniform gird; Energy conservation; Pole treatment; Concentric annuli flow; Pipe flow

1. Introduction

It is well known that energy-conservative finite difference schemes offer reliable and stable flow simulations and, in general, are preferred over non-conservative schemes when used for direct and large eddy simulations of turbulent flows. However, until recently the standard second order accurate staggered grid finite difference scheme of Harlow and Welch [1] was the only scheme that simultaneously conserved mass, momentum, and kinetic energy on a uniform mesh. A fully conservative high order accurate finite difference scheme for uniform Cartesian staggered grids was recently developed by Morinishi et al. [2]. The scheme

* Corresponding author. Tel.: +81-52-735-5346; fax: +81-52-735-5342.
E-mail addresses: youhei.morinishi@nitech.ac.jp (Y. Morinishi), Oleg.Vasilyev@Colorado.EDU (O.V. Vasilyev).

0021-9991/$ - see front matter
doi:10.1016/j.jcp.2003.12.015

conserves momentum and kinetic energy simultaneously provided that the flow is inviscid and the discrete continuity equation is satisfied.

Attempts to generalize the high order fully conservative scheme of Morinishi et al. [2] to non-uniform meshes were not fully successful. The symmetry preserving extension of the scheme proposed by Vasilyev [3] could not simultaneously conserve mass, momentum, and kinetic energy but, depending on the form of the convective term, the conservation of either momentum or energy in addition to mass was achieved. It was shown in [3] that the presence of non-zero commutation error between averaging and differencing operators in the non-uniform directions of the mesh results in non-conservation of either energy or momentum for, respectively, advective or skew-symmetric forms of the convective term. Realizing this limitation, Kajishima [4] and Ham et al. [5] were able to extend the second order fully conservative scheme of Harlow and Welch [1] to non-uniform grids by using weighted averages. However, the use of weighted averages resulted in the reduction of accuracy on non-uniform meshes.

The ultimate objective of our study is to extend the fully conservative scheme of Morinishi et al. [2] to non-uniform meshes such that both the conservation properties and high order accuracy are preserved. The general extension of the method to rectangular curvilinear coordinate system is currently underway and is based on the recognition that in order to achieve full conservation, the equations of motion should be re-written in curvilinear coordinates and the finite difference discretization should be performed in computational space (mapped curvilinear coordinates) instead of physical space (non-uniform curvilinear grid). This allows the construction of energy-conservative high order finite difference schemes on non-uniform meshes.

The common feature of orthogonal curvilinear coordinates is the presence of the pole such as the axis of symmetry in cylindrical coordinates, where, in general, the equations of motion are singular. The presence of a singularity can destroy the conservation properties of the scheme and, thus, requires special consideration. As a first step to achieve the ultimate goal of constructing fully conservative high order schemes on non-uniform meshes, we will consider cylindrical coordinates. The cylindrical coordinate system is chosen for two reasons. First, the Navier–Stokes equations written in cylindrical coordinates (x, r, θ) have a singularity at the pole, $r = 0$. Second, many important flows of physical and engineering interest are described in cylindrical coordinates, e.g. [6–8]. Eggels et al. [6] and Akselvoll and Moin [7] applied the standard staggered scheme in cylindrical coordinates. Verzicco and Orlandi [8] introduced a special technique to remove the pole singularity. However, these schemes are not energy conservative. Only the recent scheme by Fukagata and Kasagi [9] conserves energy on a uniform grid for inviscid flow. They introduced the volume-weighted interpolation proposed by Kajishima [4] and Ham et al. [5] to cylindrical coordinates.

In order to construct fully conservative schemes, the special treatment is required to remove the singularity at the pole. In particular, the radial velocity component at the pole is required for the flow simulations using the standard staggered grid configuration. The existing pole treatments are typically based on central interpolations. The pole treatments by Fukagata and Kasagi [9] and Griffin et al. [10] are single-valued and have better physical and numerical properties, while the treatment by Eggels et al. [6] is multi-valued. However, their radial velocity at the pole is not governed by the discrete radial momentum equation and, consequently, the kinetic energy is not conserved in the inviscid limit. In addition, the numerical treatment of polar coordinates by Mohseni and Colonius [11], which avoids placing a grid point at the pole, is not possible for the standard staggered grid configuration. In this work we propose to introduce a discrete radial momentum equation at the pole, which results in energy conservation. The single-valued property is satisfied through the reconstruction process.

The objectives of this work are manifold. The first objective concerns the generalization of the high order schemes of Morinishi et al. [2] to non-uniform grids in cylindrical coordinates. The second objective is to propose a novel pole treatment that in combination with the proposed scheme results in a fully conservative high order scheme.

The paper is organized as follows. The governing equations for incompressible flow in cylindrical coordinates and the corresponding transformed equations in computational space are presented in Section 2.

The conservation properties of the new formulation are discussed there as well. The radial momentum equation at the pole is introduced in Section 3. Fully conservative high order finite difference schemes in cylindrical coordinates are proposed in Section 4. In Section 5, the existing pole treatments with central interpolation are reviewed and a new pole treatment based on the radial momentum equation is proposed. Finally, in Section 6 numerical tests for energy conservation are performed for an inviscid concentric annular flow and the effect of pole treatments are studied for an inviscid pipe flow. Large eddy simulations of turbulent pipe flow demonstrate the merit of the proposed high order fully conservative scheme.

2. Governing equations and conservation properties

The governing equations for incompressible flow are the continuity and momentum equations. The governing equations for incompressible flow written in cylindrical coordinates are given by:

$$\frac{\partial u_x}{\partial x}+\frac{\partial u_r}{\partial r}+\frac{1}{r}\frac{\partial u_\theta}{\partial \theta}+\frac{u_r}{r}=0, \tag{1}$$

$$\frac{\partial u_x}{\partial t}+\frac{\partial (u_x u_x)}{\partial x}+\frac{\partial (u_r u_x)}{\partial r}+\frac{1}{r}\frac{\partial (u_\theta u_x)}{\partial \theta}+\frac{(u_r u_x)}{r}+\frac{1}{\rho}\frac{\partial p}{\partial x}=\frac{\partial \tau_{xx}}{\partial x}+\frac{\partial \tau_{rx}}{\partial r}+\frac{1}{r}\frac{\partial \tau_{\theta x}}{\partial \theta}+\frac{\tau_{rx}}{r}+f_x, \tag{2}$$

$$\begin{aligned}&\frac{\partial u_r}{\partial t}+\frac{\partial (u_x u_r)}{\partial x}+\frac{\partial (u_r u_r)}{\partial r}+\frac{1}{r}\frac{\partial (u_\theta u_r)}{\partial \theta}+\frac{(u_r u_r-u_\theta u_\theta)}{r}+\frac{1}{\rho}\frac{\partial p}{\partial r}\\ &\quad=\frac{\partial \tau_{xr}}{\partial x}+\frac{\partial \tau_{rr}}{\partial r}+\frac{1}{r}\frac{\partial \tau_{\theta r}}{\partial \theta}+\frac{(\tau_{rr}-\tau_{\theta\theta})}{r}+f_r,\end{aligned} \tag{3}$$

$$\frac{\partial u_\theta}{\partial t}+\frac{\partial (u_x u_\theta)}{\partial x}+\frac{\partial (u_r u_\theta)}{\partial r}+\frac{1}{r}\frac{\partial (u_\theta u_\theta)}{\partial \theta}+2\frac{u_r u_\theta}{r}+\frac{1}{\rho}\frac{1}{r}\frac{\partial p}{\partial \theta}=\frac{\partial \tau_{x\theta}}{\partial x}+\frac{\partial \tau_{r\theta}}{\partial r}+\frac{1}{r}\frac{\partial \tau_{\theta\theta}}{\partial \theta}+2\frac{\tau_{r\theta}}{r}+f_\theta, \tag{4}$$

where u_x, u_r and u_θ are velocity components of axial (x), radial (r) and azimuthal (θ) directions in cylindrical coordinates, f_x, f_r, and f_θ are body force components, ρ is the density, and p is the pressure. The components of the viscous tensor, τ_{ij} $(i,j=x,r,\theta)$ for the Newtonian fluid are given by

$$\tau_{xx}=2\nu\left(\frac{\partial u_x}{\partial x}\right),\quad \tau_{rr}=2\nu\left(\frac{\partial u_r}{\partial r}\right),\quad \tau_{\theta\theta}=2\nu\left(\frac{1}{r}\frac{\partial u_\theta}{\partial \theta}+\frac{u_r}{r}\right),\quad \tau_{xr}=\tau_{rx}=\nu\left(\frac{\partial u_r}{\partial x}+\frac{\partial u_x}{\partial r}\right),$$
$$\tau_{x\theta}=\tau_{\theta x}=\nu\left(\frac{\partial u_\theta}{\partial x}+\frac{1}{r}\frac{\partial u_x}{\partial \theta}\right),\quad \tau_{r\theta}=\tau_{\theta r}=\nu\left(\frac{\partial u_\theta}{\partial r}-\frac{u_\theta}{r}+\frac{1}{r}\frac{\partial u_r}{\partial \theta}\right).$$

Many finite difference schemes in cylindrical coordinates have been constructed in physical space, e.g. [6–8]. On the other hand, the mapping of independent variables is a useful tool for constructing finite difference schemes on non-uniform grids. In this study, (x,r,θ) coordinates in physical space are, respectively, mapped into $(\zeta^x,\zeta^r,\zeta^\theta)$ in computational space as

$$x=x(\zeta^x),\quad r=r(\zeta^r),\quad \theta=\theta(\zeta^\theta) \tag{5}$$

and

$$\zeta^x=\zeta^x(x),\quad \zeta^r=\zeta^r(r),\quad \zeta^\theta=\zeta^\theta(\theta). \tag{6}$$

For instance, the mapping of the r–θ plane including the pole onto the ζ^r–ζ^θ plane is shown in Fig. 1 for the case of $N_r=4$ and $N_\theta=8$. Scaling factors and the Jacobian are defined as

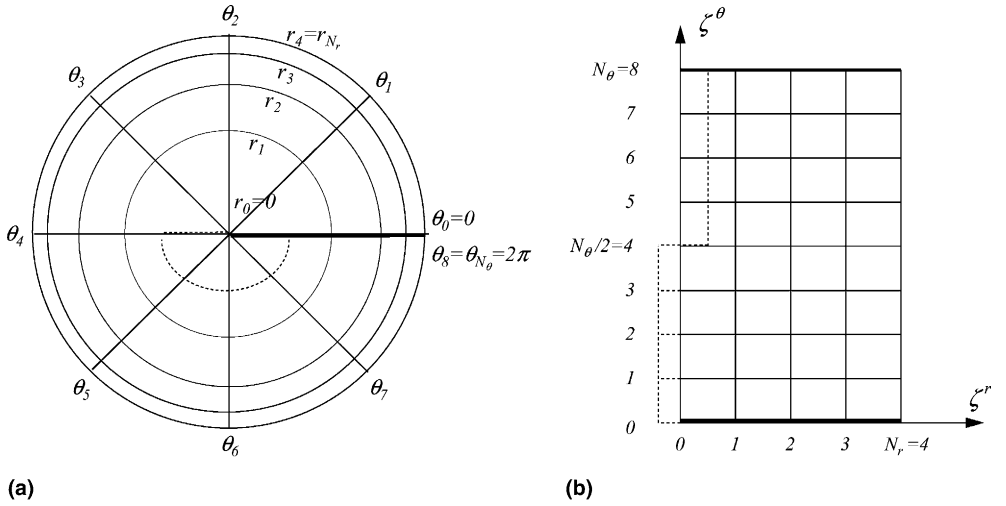

Fig. 1. Mapping of (a) r–θ plane onto (b) ζ^r–ζ^θ plane for $N_r = 4$ and $N_\theta = 8$.

$$h_x = \frac{\mathrm{d}x}{\mathrm{d}\zeta^x}, \quad h_r = \frac{\mathrm{d}r}{\mathrm{d}\zeta^r}, \quad h_\theta = r\frac{\mathrm{d}\theta}{\mathrm{d}\zeta^\theta}, \quad J = h_x h_r h_\theta = r\frac{\mathrm{d}x}{\mathrm{d}\zeta^x}\frac{\mathrm{d}r}{\mathrm{d}\zeta^r}\frac{\mathrm{d}\theta}{\mathrm{d}\zeta^\theta}. \tag{7}$$

The derivatives in physical space are transformed into computational space as

$$\frac{\partial}{\partial x} = \frac{1}{h_x}\frac{\partial}{\partial \zeta^x}, \quad \frac{\partial}{\partial r} = \frac{1}{h_r}\frac{\partial}{\partial \zeta^r}, \quad \frac{1}{r}\frac{\partial}{\partial \theta} = \frac{1}{h_\theta}\frac{\partial}{\partial \zeta^\theta}. \tag{8}$$

In addition to the derivative mapping, we can use the following relations for equation transformation:

$$\frac{1}{J}\frac{\partial}{\partial \zeta^x}\left(\frac{J}{h_x}\right) = 0, \quad \frac{1}{J}\frac{\partial}{\partial \zeta^r}\left(\frac{J}{h_r}\right) = \frac{1}{r}, \quad \frac{1}{J}\frac{\partial}{\partial \zeta^\theta}\left(\frac{J}{h_\theta}\right) = 0. \tag{9}$$

Finally, the transformed continuity and momentum equations can be written as

$$(\mathrm{Cont.}) \equiv \frac{1}{J}\frac{\partial}{\partial \zeta^j}\left[\frac{J}{h_j}u_j\right] = 0, \tag{10}$$

$$\frac{\partial u_x}{\partial t} + \frac{1}{J}\frac{\partial}{\partial \zeta^j}\left[\frac{J}{h_j}u_j u_x\right] + \frac{1}{\rho}\frac{1}{h_x}\frac{\partial p}{\partial \zeta^x} = \frac{1}{h_j}\frac{\partial \tau_{jx}}{\partial \zeta^j} + \frac{\tau_{rx}}{r} + f_x, \tag{11}$$

$$\frac{\partial u_r}{\partial t} + \frac{1}{J}\frac{\partial}{\partial \zeta^j}\left[\frac{J}{h_j}u_j u_r\right] - \frac{u_\theta u_\theta}{r} + \frac{1}{\rho}\frac{1}{h_r}\frac{\partial p}{\partial \zeta^r} = \frac{1}{h_j}\frac{\partial \tau_{jr}}{\partial \zeta^j} + \frac{(\tau_{rr} - \tau_{\theta\theta})}{r} + f_r, \tag{12}$$

$$\frac{\partial u_\theta}{\partial t} + \frac{1}{J}\frac{\partial}{\partial \zeta^j}\left[\frac{J}{h_j}u_j u_\theta\right] + \frac{u_r u_\theta}{r} + \frac{1}{\rho}\frac{1}{h_\theta}\frac{\partial p}{\partial \zeta^\theta} = \frac{1}{h_j}\frac{\partial \tau_{j\theta}}{\partial \zeta^j} + 2\frac{\tau_{r\theta}}{r} + f_\theta. \tag{13}$$

The repeated indices, for instance, j, imply the summation over $j = x, r, \theta$. In addition, the index for the scaling factor moves with the accompanying derivative index. The formulation using the Jacobian was first introduced by Vinokur [12]. In this study, we will construct a fully conservative finite difference scheme in

cylindrical coordinates for incompressible flow based on Eqs. (10)–(13), which implies that all spatial discrete operations are done in the computational space. The pressure term in the momentum equation can be represented symbolically as

$$(\text{Pres.})_i = \frac{1}{\rho}\frac{1}{h_i}\frac{\partial p}{\partial \zeta^i}. \tag{14}$$

The convective term in the momentum equation can be written in the divergence, advective, or skew-symmetric forms. The divergence form, $(\text{Div.})_i$, is defined as

$$(\text{Div.})_x = \frac{1}{J}\frac{\partial}{\partial \zeta^j}\left[\frac{J}{h_j}u_j u_x\right], \tag{15}$$

$$(\text{Div.})_r = \frac{1}{J}\frac{\partial}{\partial \zeta^j}\left[\frac{J}{h_j}u_j u_r\right] - \frac{u_\theta u_\theta}{r}, \tag{16}$$

$$(\text{Div.})_\theta = \frac{1}{J}\frac{\partial}{\partial \zeta^j}\left[\frac{J}{h_j}u_j u_\theta\right] + \frac{u_r u_\theta}{r}. \tag{17}$$

The advective form, $(\text{Adv.})_i$, is given by

$$(\text{Adv.})_x = \frac{u_j}{h_j}\frac{\partial u_x}{\partial \zeta^j}, \tag{18}$$

$$(\text{Adv.})_r = \frac{u_j}{h_j}\frac{\partial u_r}{\partial \zeta^j} - \frac{u_\theta u_\theta}{r}, \tag{19}$$

$$(\text{Adv.})_\theta = \frac{u_j}{h_j}\frac{\partial u_\theta}{\partial \zeta^j} + \frac{u_r u_\theta}{r}. \tag{20}$$

The skew-symmetric form, $(\text{Skew.})_i$, is defined as the average of the divergence and advective forms:

$$(\text{Skew.})_i = \frac{1}{2}(\text{Div.})_i + \frac{1}{2}(\text{Adv.})_i. \tag{21}$$

The three forms, $(\text{Div.})_i$, $(\text{Adv.})_i$, and $(\text{Skew.})_i$, are commutable with the following identities, provided that the continuity constraint is satisfied:

$$(\text{Div.})_i = (\text{Adv.})_i + u_i(\text{Cont.}), \tag{22}$$

$$(\text{Skew.})_i = (\text{Div.})_i - \frac{1}{2}u_i(\text{Cont.}) = (\text{Adv.})_i + \frac{1}{2}u_i(\text{Cont.}). \tag{23}$$

Next, conservation properties for the momentum and the kinetic energy in cylindrical coordinates are briefly reviewed. The term written in a form, $(1/J)(\partial\phi/\partial\zeta^j)$ (hereafter referred as divergence form), is conservative in the computational space, since the Gauss theorem is accomplished in the following way:

$$\int_V \left(\frac{1}{J}\frac{\partial \phi}{\partial \zeta^j}\right) \mathrm{d}V = \int_V \frac{\partial \phi}{\partial \zeta^j}\, \mathrm{d}\zeta^x\, \mathrm{d}\zeta^r\, \mathrm{d}\zeta^\theta = \int_{S^j} \phi\, \mathrm{d}S^j, \tag{24}$$

where $\mathrm{d}V = J\,\mathrm{d}\zeta^x\,\mathrm{d}\zeta^r\,\mathrm{d}\zeta^\theta$ and $\mathrm{d}S^j = \mathrm{d}\zeta^x\,\mathrm{d}\zeta^r\,\mathrm{d}\zeta^\theta/\mathrm{d}\zeta^j$. Consequently, any term written in the divergence form is conserved a priori. It should be noted, that the momentum equations (2)–(4) or the transformed mo-

mentum equations (11)–(13), in addition to the terms written in divergence form, have source terms such as $u_\theta u_\theta/r$ or $u_r u_\theta/r$. These source terms, analogously to the body force components, contribute to the overall momentum balance and energy exchange. However, these terms are physical and reflect the curvature of the curvilinear coordinate system. Consequently, conservation properties of the finite different schemes should be studied in light of their analytical counterparts, i.e. the terms written in divergence form should be conserved, while the source terms in the discrete equations should contribute to the overall momentum and energy balance the same way as in the continuous case.

The kinetic energy is defined as $K = (1/2)u_i u_i = (1/2)(u_x^2 + u_r^2 + u_\theta^2)$. The transport equation for K for inviscid flow without the body force is

$$\frac{\partial K}{\partial t} + u_i(\text{Div.})_i + u_i(\text{Pres.})_i = 0. \tag{25}$$

The pressure term in the energy equation is reformed as follows:

$$u_i(\text{Pres.})_i = \frac{1}{J}\frac{\partial}{\partial \zeta^i}\left[\frac{J}{h_i}u_i p\right] - p\ (\text{Cont.}). \tag{26}$$

The convective term with the divergence form in the energy equation can be rewritten as follows:

$$u_i(\text{Div.})_i = \frac{1}{J}\frac{\partial}{\partial \zeta^j}\left[\frac{J}{h_j}u_j K\right] + K\ (\text{Cont.}). \tag{27}$$

In the same manner, the advective and skew-symmetric forms of the convective term have, respectively, the following forms in the energy equation:

$$u_i(\text{Adv.})_i = \frac{1}{J}\frac{\partial}{\partial \zeta^j}\left[\frac{J}{h_j}u_j K\right] - K\ (\text{Cont.}), \tag{28}$$

$$u_i(\text{Skew.})_i = \frac{1}{J}\frac{\partial}{\partial \zeta^j}\left[\frac{J}{h_j}u_j K\right]. \tag{29}$$

Therefore, the convective term written in the skew-symmetric form is conservative a priori, and the other convection forms and the pressure terms are conservative, provided that the continuity constraint is satisfied. Thus, the kinetic energy is conserved in the inviscid flow limit in the absence of the body force f_i. This energy conservation should be preserved for the energy conserving scheme.

3. Radial momentum equation at the pole

In this section, the momentum equation for the radial velocity component is considered at the pole, since the component is defined at the pole in the standard staggered grid configuration. Here we select the cylindrical coordinate system as $x = x$, $y = r\cos\theta$ and $z = r\sin\theta$. Corresponding transformation for the vector components between r–θ and y–z planes is given by

$$u_r = u_y\cos\theta + u_z\sin\theta, \tag{30}$$

$$u_\theta = -u_y\sin\theta + u_z\cos\theta. \tag{31}$$

In the same manner the transformation for the tensor components are

$$\tau_{rr} = \tau_{yy}\cos^2\theta + \tau_{zz}\sin^2\theta + \tau_{yz}\sin 2\theta, \tag{32}$$

$$\tau_{\theta\theta} = \tau_{yy}\sin^2\theta + \tau_{zz}\cos^2\theta - \tau_{yz}\sin 2\theta, \tag{33}$$

$$\tau_{\theta r} = \tau_{r\theta} = \tau_{yz}\cos 2\theta - \frac{1}{2}(\tau_{yy} - \tau_{zz})\sin 2\theta. \tag{34}$$

Using the single-valued property at the pole for the velocity and tensor components in Cartesian coordinates, we get

$$\frac{\partial u_r}{\partial\theta} = u_\theta, \quad \frac{\partial u_\theta}{\partial\theta} = -u_r \quad \text{at } r = 0, \tag{35}$$

$$\frac{\partial\tau_{\theta r}}{\partial\theta} + \tau_{rr} - \tau_{\theta\theta} = 0 \quad \text{at } r = 0. \tag{36}$$

The relation of Eq. (35) was pointed out by Constantinescu and Lele [13]. These relations are effectively used for singularity removal with the aid of L'Hopital's theorem:

$$\lim_{r=0}\tau_{\theta r} = \nu\frac{\partial}{\partial\theta}\left(\frac{\partial u_r}{\partial r}\right), \tag{37}$$

$$\lim_{r=0}\frac{1}{r}\left(\frac{\partial\tau_{\theta r}}{\partial\theta} + \tau_{rr} - \tau_{\theta\theta}\right) = \frac{\partial}{\partial r}\left(\frac{\partial\tau_{\theta r}}{\partial\theta} + \tau_{rr} - \tau_{\theta\theta}\right). \tag{38}$$

Eq. (37) will be adopted for $\tau_{\theta r}$ at the pole in the discrete equations. The radial momentum equation, Eq. (3), is rewritten at the pole with the aid of Eq. (38) as

$$\begin{aligned}&\frac{\partial u_r}{\partial t} + \frac{\partial(u_x u_r)}{\partial x} + \frac{\partial(u_r u_r)}{\partial r} + \frac{\partial}{\partial r}\left(\frac{\partial u_\theta u_r}{\partial\theta} + u_r u_r - u_\theta u_\theta\right) + \frac{1}{\rho}\frac{\partial p}{\partial r}\\ &\quad = \frac{\partial\tau_{xr}}{\partial x} + \frac{\partial\tau_{rr}}{\partial r} + \frac{\partial}{\partial r}\left(\frac{\partial\tau_{\theta r}}{\partial\theta} + \tau_{rr} - \tau_{\theta\theta}\right) + f_r \quad \text{at } r = 0,\end{aligned} \tag{39}$$

where the convection term is also rewritten in the same manner as Eq. (38). The above radial momentum equation reconfirms that the singularity at the pole is not physical but coordinate originated, and it should be used in future numerical and analytical studies. However in this study, the singularity removal is adopted only for the viscous term, since the singularity on the convection term will be removed to satisfy the energy conservation in the corresponding discrete equation. Thus, the radial momentum equation at the pole, which we use in this study, is given by

$$\frac{\partial u_r}{\partial t} + \frac{1}{J}\frac{\partial}{\partial\zeta^j}\left[\frac{J}{h_j}u_j u_r\right] - \frac{u_\theta u_\theta}{r} + \frac{1}{\rho}\frac{1}{h_r}\frac{\partial p}{\partial\zeta^r} = \frac{1}{h_x}\frac{\partial\tau_{xr}}{\partial\zeta^x} + \frac{1}{h_r}\frac{\partial\tau_{rr}}{\partial\zeta^r} + \frac{1}{h_r}\frac{\partial}{\partial\zeta^r}\left(\frac{\partial\tau_{\theta r}}{\partial\theta} + \tau_{rr} - \tau_{\theta\theta}\right) + f_r \quad \text{at } r = 0. \tag{40}$$

4. Fully conservative finite difference schemes in cylindrical coordinates

4.1. Second order finite difference scheme

In this study we propose the following scheme as the second order accurate finite difference scheme for the continuity and momentum equations in cylindrical coordinates. Definition points for the velocity components and pressure are specified in Fig. 2. The pressure is defined at the center of each cell,

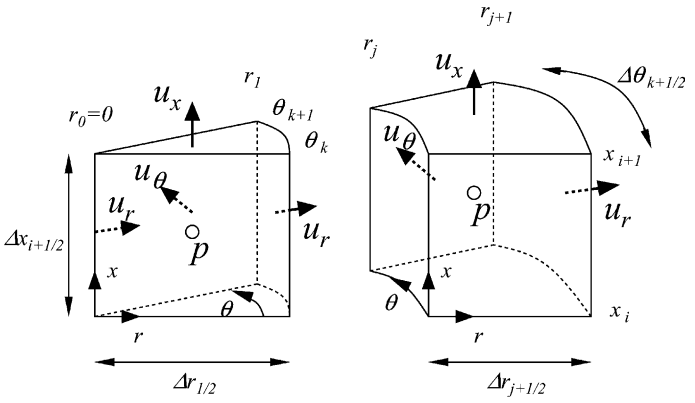

Fig. 2. Definition points for the velocity components and pressure.

$(x_{i+1/2}, r_{j+1/2}, \theta_{k+1/2})$, while the velocity components in the axial, radial and azimuthal directions are defined at $(x_i, r_{j+1/2}, \theta_{k+1/2})$, $(x_{i+1/2}, r_j, \theta_{k+1/2})$ and $(x_{i+1/2}, r_{j+1/2}, \theta_k)$, respectively, as the standard staggered configuration. Fig. 3 shows the staggered grid arrangement in the ζ^r–ζ^θ plane corresponding to Fig. 1(b). In particular, the radial velocity is also defined at the pole, $(x_{i+1/2}, 0, \theta_{k+1/2})$. The continuity equation is discretized at the pressure point, while the components of the momentum equation are discretized at the corresponding velocity points:

$$(\text{Cont.-2}) = 0, \tag{41}$$

$$\frac{\partial u_x}{\partial t} + (\text{Conv.-2})_x + (\text{Pres.-2})_x = \frac{1}{h_j}\frac{\delta_1}{\delta_1\ \zeta^j}\tau_{jx} + \frac{1}{\overline{J}^{1\zeta^x}}\overline{\left(\frac{J}{r}\tau_{rx}\right)}^{1\ \zeta^x} + f_x, \tag{42}$$

$$\frac{\partial u_r}{\partial t} + (\text{Conv.-2})_r + (\text{Pres.-2})_r = \frac{1}{h_j}\frac{\delta_1}{\delta_1\ \zeta^j}\tau_{jr} + \frac{1}{\overline{J}^{1\zeta^r}}\overline{\left(\frac{J}{r}(\tau_{rr} - \tau_{\theta\theta})\right)}^{1\ \zeta^r} + f_r, \tag{43}$$

$$\frac{\partial u_\theta}{\partial t} + (\text{Conv.-2})_\theta + (\text{Pres.-2})_\theta = \frac{1}{h_j}\frac{\delta_1}{\delta_1\ \zeta^j}\tau_{j\theta} + \frac{2}{\overline{J}^{1\zeta^\theta}}\overline{\left(\frac{J}{r}\tau_{r\theta}\right)}^{1\ \zeta^\theta} + f_\theta, \tag{44}$$

where "-2" denotes a second order accurate approximation on a staggered grid in cylindrical coordinates. Here, we suppose that the components of the viscous tensor are given at the required discrete points. In the proposed finite difference scheme, all the discrete operations are done in the computational space. Spatial discrete operators in the computational space are defined in Appendix A. The definitions of *local* and *global* discrete conservation is given there as well. The finite difference approximations for the continuity and pressure terms can be written as follows:

$$(\text{Cont.-2}) = \frac{1}{J}\frac{\delta_1}{\delta_1\ \zeta^j}\left[\frac{J}{h_j}u_j\right] \quad (= 0), \tag{45}$$

$$(\text{Pres.-2})_i = \frac{J}{\overline{J}^{1\zeta^i}}\frac{1}{\rho}\frac{1}{h_i}\frac{\delta_1}{\delta_1\ \zeta^i}p. \tag{46}$$

$(\text{Conv.-2})_i$ is a generic form of the convection term and three forms are possible as in Morinishi et al. [2].

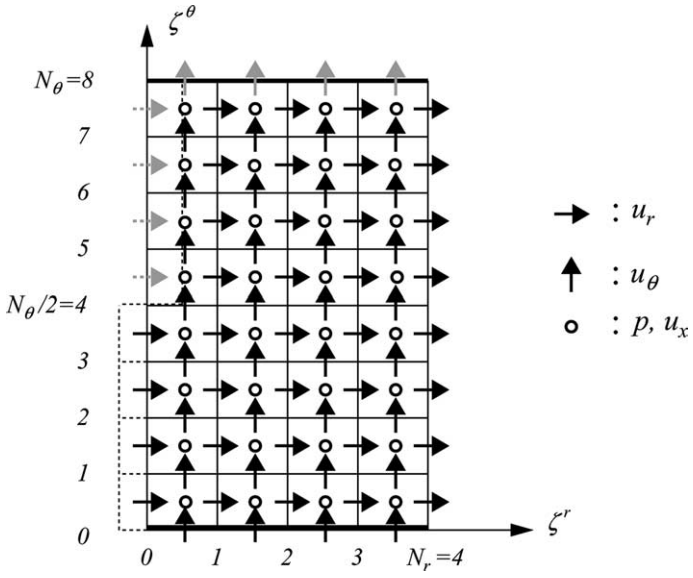

Fig. 3. Staggered grid configuration in ζ^r–ζ^θ plane.

Divergence form:

$$(\text{Div.-2})_x = \frac{1}{\overline{J}^{1\zeta^x}} \frac{\delta_1}{\delta_1\ \zeta^j} \left[\overline{\left(\frac{J}{h_j} u_j\right)}^{1\zeta^x} \overline{u_x}^{1\zeta^j} \right], \tag{47}$$

$$(\text{Div.-2})_r = \frac{1}{\overline{J}^{1\zeta^r}} \frac{\delta_1}{\delta_1\ \zeta^j} \left[\overline{\left(\frac{J}{h_j} u_j\right)}^{1\ \zeta^r} \overline{u_r}^{1\ \zeta^j} \right] - \frac{1}{\overline{J}^{1\zeta^r}} \overline{\left(\frac{J}{r} \overline{u_\theta}^{1\zeta^\theta} \overline{u_\theta}^{1\zeta^\theta}\right)}^{1\ \zeta^r}, \tag{48}$$

$$(\text{Div.-2})_\theta = \frac{1}{\overline{J}^{1\zeta^\theta}} \frac{\delta_1}{\delta_1\ \zeta^j} \left[\overline{\left(\frac{J}{h_j} u_j\right)}^{1\ \zeta^\theta} \overline{u_\theta}^{1\ \zeta^j} \right] + \frac{1}{\overline{J}^{1\zeta^\theta}} \overline{\left(\frac{J}{r} \overline{u_r}^{1\zeta^r} \overline{u_\theta}^{1\zeta^\theta}\right)}^{1\ \zeta^\theta}. \tag{49}$$

Advective form:

$$(\text{Adv.-2})_x = \frac{1}{\overline{J}^{1\zeta^x}} \overline{\left[\overline{\left(\frac{J}{h_j} u_j\right)}^{1\zeta^x} \frac{\delta_1\ u_x}{\delta_1\ \zeta^j} \right]}^{1\zeta^j}, \tag{50}$$

$$(\text{Adv.-2})_r = \frac{1}{\overline{J}^{1\zeta^r}} \overline{\left[\overline{\left(\frac{J}{h_j} u_j\right)}^{1\zeta^r} \frac{\delta_1\ u_r}{\delta_1\ \zeta^j} \right]}^{1\zeta^j} - \frac{1}{\overline{J}^{1\zeta^r}} \overline{\left(\frac{J}{r} \overline{u_\theta}^{1\zeta^\theta} \overline{u_\theta}^{1\zeta^\theta}\right)}^{1\ \zeta^r}, \tag{51}$$

$$(\text{Adv.-2})_\theta = \frac{1}{\overline{J}^{1\zeta^\theta}} \overline{\left[\overline{\left(\frac{J}{h_j} u_j\right)}^{1\zeta^\theta} \frac{\delta_1\ u_\theta}{\delta_1\ \zeta^j} \right]}^{1\zeta^j} + \frac{1}{\overline{J}^{1\zeta^\theta}} \overline{\left(\frac{J}{r} \overline{u_r}^{1\zeta^r} \overline{u_\theta}^{1\zeta^\theta}\right)}^{1\ \zeta^\theta}. \tag{52}$$

Skew-symmetric form:

$$(\text{Skew.-2})_i = \frac{1}{2}(\text{Div.-2})_i + \frac{1}{2}(\text{Adv.-2})_i. \tag{53}$$

Note that the divergence form of the convective term is conserved a priori in the momentum equation in the light of momentum conservation discussed in Section 2. The three discrete convection forms are commutable with the following identities provided that the discrete continuity equation is satisfied:

$$(\text{Div.-2})_i = (\text{Adv.-2})_i + u_i \frac{1}{\overline{J}^{1\zeta^i}} \overline{J\ (\text{Cont.-2})}^{1\zeta^i}, \tag{54}$$

$$(\text{Skew.-2})_i = (\text{Div.-2})_i - \frac{1}{2} u_i \frac{1}{\overline{J}^{1\zeta^i}} \overline{J\ (\text{Cont.-2})}^{1\zeta^i} = (\text{Adv.-2})_i + \frac{1}{2} u_i \frac{1}{\overline{J}^{1\zeta^i}} \overline{J\ (\text{Cont.-2})}^{1\zeta^i}. \tag{55}$$

Now we shall show the energy conservation property of the proposed finite difference scheme. To estimate the energy conservation, a discrete kinetic energy norm defined at the pressure point is introduced for the second order accurate discretization.

$$K_{2\text{nd}} = \frac{1}{2J} \overline{\overline{J}^{1\zeta^i} u_i u_i}^{1\zeta^i} = \frac{1}{2J} \left[\overline{\overline{J}^{1\zeta^x} u_x u_x}^{1\zeta^x} + \overline{\overline{J}^{1\zeta^r} u_r u_r}^{1\zeta^r} + \overline{\overline{J}^{1\zeta^\theta} u_\theta u_\theta}^{1\zeta^\theta} \right] \tag{56}$$

The corresponding discrete kinetic energy equation for inviscid flow without the body force can be written as

$$\frac{\partial K_{2\text{nd}}}{\partial t} + \frac{1}{J} \overline{\overline{J}^{1\zeta^i} u_i (\text{Conv.-2})_i}^{1\zeta^i} + \frac{1}{J} \overline{\overline{J}^{1\zeta^i} u_i (\text{Pres.-2})_i}^{1\zeta^i} = 0. \tag{57}$$

The pressure term in the energy equation is conservative, provided that the discrete continuity is satisfied:

$$\frac{1}{J} \overline{\overline{J}^{1\zeta^i} u_i (\text{Pres.-2})_i}^{1\zeta^i} = \frac{1}{\rho} \frac{1}{J} \frac{\delta_1}{\delta_1 \zeta^i} \left[\left(\frac{J}{h_i} u_i \right) \overline{p}^{1\zeta^i} \right] - \frac{p}{\rho} (\text{Cont.-2}). \tag{58}$$

The conservation property of the skew-symmetric form is proved as follows:

$$\begin{aligned} \frac{1}{J} \overline{\overline{J}^{1\zeta^i} u_i (\text{Skew.-2})_i}^{1\zeta^i} = {} & \frac{1}{J} \frac{\delta_1}{\delta_1 \zeta^j} \left[\overline{\left(\frac{J}{h_j} u_j \right)^{1\zeta^i} \frac{1}{2} \widetilde{(u_i u_i)}^{1\zeta^j}}^{1\zeta^i} \right] - \frac{1}{J} \overline{u_r \overline{\left(\frac{J}{r} \overline{u_\theta}^{1\zeta^\theta} \overline{u_\theta}^{1\zeta^\theta} \right)}^{1\zeta^r}}^{1\zeta^r} \\ & + \frac{1}{J} \overline{u_\theta \overline{\left(\frac{J}{r} \overline{u_r}^{1\zeta^r} \overline{u_\theta}^{1\zeta^\theta} \right)}^{1\zeta^\theta}}^{1\zeta^\theta}. \end{aligned} \tag{59}$$

The first term on the right-hand side of Eq. (59) is locally conservative. The sum of the second and third terms over a periodic or zero-bounded domain is rewritten as (see Appendix A)

$$\begin{aligned} & \sum \frac{1}{J} \left[- \overline{u_r \overline{\left(\frac{J}{r} \overline{u_\theta}^{1\zeta^\theta} \overline{u_\theta}^{1\zeta^\theta} \right)}^{1\zeta^r}}^{1\zeta^r} + \overline{u_\theta \overline{\left(\frac{J}{r} \overline{u_r}^{1\zeta^r} \overline{u_\theta}^{1\zeta^\theta} \right)}^{1\zeta^\theta}}^{1\zeta^\theta} \right] \left(J \Delta\zeta^x \Delta\zeta^r \Delta\zeta^\theta \right) \\ & = \sum \frac{1}{r} \left[- \overline{u_r}^{1\zeta^r} \overline{u_\theta}^{1\zeta^\theta} \overline{u_\theta}^{1\zeta^\theta} + \overline{u_\theta}^{1\zeta^\theta} \overline{u_r}^{1\zeta^r} \overline{u_\theta}^{1\zeta^\theta} \right] \left(J \Delta\zeta^x \Delta\zeta^r \Delta\zeta^\theta \right) = 0. \end{aligned} \tag{60}$$

Therefore, the sum of the second and third terms in the skew-symmetric form is globally conservative in the energy equation. Conservation properties for the divergence and advective forms are the same as that for the skew-symmetric form, which follows from the commutability equation (55). In summary, the proposed finite difference scheme satisfies the conservation property as discussed in Section 2 in a discrete sense even for non-uniform meshes, i.e. the scheme is fully conservative in cylindrical coordinates on a non-uniform grid.

This study assumes that a temporal discretization error is negligible for the energy conservation property. We will introduce a third order Runge–Kutta time marching method for the inviscid part. Energy-conservative temporal discretization by Ham et al. [5] can be combined with the present spatial discretization method with the energy norm of Eq. (56), although a non-linear implicit discrete system should be solved at each time step.

The Jacobian and scaling factors are approximated as

$$h_x = \Delta x, \quad h_r = \Delta r, \quad h_\theta = r\Delta\theta, \quad J = r\Delta x\Delta r\Delta\theta, \tag{61}$$

with $\Delta\zeta^x = \Delta\zeta^r = \Delta\zeta^\theta = 1$, where Δx, Δr and $\Delta\theta$ are grid spacings at the defined point in the physical space, respectively. The averaged Jacobian, $\overline{J}^{1\zeta_i}$, which appeared in the discrete equations, can be replaced by J for simulations with computational region, which does not include $r = 0$.

4.2. Mixed high and second order finite difference scheme

The azimuthal grid width is proportional to the radius for standard grid configuration in cylindrical coordinates. Therefore, high order finite difference schemes in the azimuthal direction may be useful for large eddy simulations in a pipe. In this section, a mixed high (x–θ) and second (r) order energy conservative finite difference scheme is presented. The discrete form for continuity and pressure terms are

$$(\text{Cont.-}n\cdot 2\cdot n) = \frac{1}{J}\sum_{\ell=1}^{n/2}\alpha_\ell \frac{\delta_{(2\ell-1)}}{\delta_{(2\ell-1)}\ \zeta^x}\left[\frac{J}{h_x}u_x\right] + \frac{1}{J}\frac{\delta_1}{\delta_1\ \zeta^r}\left[\frac{J}{h_r}u_r\right] + \frac{1}{J}\sum_{\ell=1}^{n/2}\alpha_\ell \frac{\delta_{(2\ell-1)}}{\delta_{(2\ell-1)}\ \zeta^\theta}\left[\frac{J}{h_\theta}u_\theta\right] = 0, \tag{62}$$

$$(\text{Pres.-}n\cdot 2\cdot n)_x = \frac{J}{\overline{J}^{1\zeta^x}}\frac{1}{\rho}\frac{1}{h_x}\sum_{\ell=1}^{n/2}\alpha_\ell \frac{\delta_{(2\ell-1)}\ p}{\delta_{(2\ell-1)}\ \zeta^x}, \tag{63}$$

$$(\text{Pres.-}n\cdot 2\cdot n)_r = \frac{J}{\overline{J}^{1\zeta^r}}\frac{1}{\rho}\frac{1}{h_r}\frac{\delta_1\ p}{\delta_1\ \zeta^r}, \tag{64}$$

$$(\text{Pres.-}n\cdot 2\cdot n)_\theta = \frac{J}{\overline{J}^{1\zeta^\theta}}\frac{1}{\rho}\frac{1}{h_\theta}\sum_{\ell=1}^{n/2}\alpha_\ell \frac{\delta_{(2\ell-1)}\ p}{\delta_{(2\ell-1)}\ \zeta^\theta}, \tag{65}$$

where the α_ℓ are the interpolation weights and given as the solution of the following linear system:

$$\sum_{\ell=1}^{n/2}(2\ell-1)^{2(i-1)}\alpha_\ell = \delta_{i1}, \quad i = 1,2,\ldots,n/2. \tag{66}$$

The weights up to $n = 12$ are summarized in Table 1. The components of the convection scheme written in divergence form are:

Table 1
Weights for nth order interpolations

n	α_1	α_2	α_3	α_4	α_5	α_6
2	+1	0	0	0	0	0
4	$+\frac{9}{8}$	$-\frac{1}{8}$	0	0	0	0
6	$+\frac{150}{128}$	$-\frac{25}{128}$	$+\frac{3}{128}$	0	0	0
8	$+\frac{1225}{1024}$	$-\frac{245}{1024}$	$+\frac{49}{1024}$	$-\frac{5}{1024}$	0	0
10	$+\frac{39,690}{32,768}$	$-\frac{8820}{32,768}$	$+\frac{2268}{32,768}$	$-\frac{405}{32,768}$	$+\frac{35}{32,768}$	0
12	$+\frac{320,166}{262,144}$	$-\frac{76,230}{262,144}$	$+\frac{22,869}{262,144}$	$-\frac{5445}{262,144}$	$+\frac{847}{262,144}$	$-\frac{63}{262,144}$

$$(\text{Div.-}n\cdot 2\cdot n)_x = \frac{1}{\overline{J}^{1\zeta^x}}\sum_{\ell=1}^{n/2}\alpha_\ell\frac{\delta_{(2\ell-1)}}{\delta_{(2\ell-1)}\ \zeta^x}\left[\overline{\left(\frac{J}{h_x}u_x\right)}^{n\text{th}\ \zeta^x}\ \overline{u_x}^{(2\ell-1)\zeta^x}\right]+\frac{1}{\overline{J}^{1\zeta^x}}\frac{\delta_1}{\delta_1\ \zeta^r}\left[\overline{\left(\frac{J}{h_r}u_r\right)}^{n\text{th}\ \zeta^x}\ \overline{u_x}^{1\zeta^r}\right]$$
$$+\frac{1}{\overline{J}^{1\zeta^x}}\sum_{\ell=1}^{n/2}\alpha_\ell\frac{\delta_{(2\ell-1)}}{\delta_{(2\ell-1)}\ \zeta^\theta}\left[\overline{\left(\frac{J}{h_\theta}u_\theta\right)}^{n\text{th}\ \zeta^x}\ \overline{u_x}^{(2\ell-1)\zeta^\theta}\right], \tag{67}$$

$$(\text{Div.-}n\cdot 2\cdot n)_r = \frac{1}{\overline{J}^{1\zeta^r}}\sum_{\ell=1}^{n/2}\alpha_\ell\frac{\delta_{(2\ell-1)}}{\delta_{(2\ell-1)}\ \zeta^x}\left[\overline{\left(\frac{J}{h_x}u_x\right)}^{1\ \zeta^r}\ \overline{u_r}^{(2\ell-1)\zeta^x}\right]+\frac{1}{\overline{J}^{1\zeta^r}}\frac{\delta_1}{\delta_1\ \zeta^r}\left[\overline{\left(\frac{J}{h_r}u_r\right)}^{1\ \zeta^r}\ \overline{u_r}^{1\ \zeta^r}\right]$$
$$+\frac{1}{\overline{J}^{1\zeta^r}}\sum_{\ell=1}^{n/2}\alpha_\ell\frac{\delta_{(2\ell-1)}}{\delta_{(2\ell-1)}\ \zeta^\theta}\left[\overline{\left(\frac{J}{h_\theta}u_\theta\right)}^{1\ \zeta^r}\ \overline{u_r}^{(2\ell-1)\zeta^\theta}\right]-\frac{1}{\overline{J}^{1\zeta^r}}\overline{\left(\frac{J}{r}\ \overline{u_\theta}^{n\text{th}\ \zeta^\theta}\ \overline{u_\theta}^{n\text{th}\ \zeta^\theta}\right)}^{1\ \zeta^r}, \tag{68}$$

$$(\text{Div.-}n\cdot 2\cdot n)_\theta = \frac{1}{\overline{J}^{1\zeta^\theta}}\sum_{\ell=1}^{n/2}\alpha_\ell\frac{\delta_{(2\ell-1)}}{\delta_{(2\ell-1)}\ \zeta^x}\left[\overline{\left(\frac{J}{h_x}u_x\right)}^{n\text{th}\ \zeta^\theta}\ \overline{u_\theta}^{(2\ell-1)\ \zeta^x}\right]+\frac{1}{\overline{J}^{1\zeta^\theta}}\frac{\delta_1}{\delta_1\ \zeta^r}\left[\overline{\left(\frac{J}{h_r}u_r\right)}^{n\text{th}\ \zeta^\theta}\ \overline{u_\theta}^{1\ \zeta^r}\right]$$
$$+\frac{1}{\overline{J}^{1\zeta^\theta}}\sum_{\ell=1}^{n/2}\alpha_\ell\frac{\delta_{(2\ell-1)}}{\delta_{(2\ell-1)}\ \zeta^\theta}\left[\overline{\left(\frac{J}{h_\theta}u_\theta\right)}^{n\text{th}\ \zeta^\theta}\ \overline{u_\theta}^{(2\ell-1)\ \zeta^\theta}\right]+\frac{1}{\overline{J}^{1\zeta^\theta}}\overline{\left(\frac{J}{r}\ \overline{u_r}^{1\zeta^r}\ \overline{u_\theta}^{n\text{th}\ \zeta^\theta}\right)}^{n\text{th}\ \zeta^\theta}, \tag{69}$$

where $\overline{\phi}^{n\text{th}\ \zeta^x}$ and $\overline{\phi}^{n\text{th}\ \zeta^\theta}$ are the nth order interpolations that are defined, respectively, as

$$\overline{\phi}^{n\text{th}\ \zeta^x}=\sum_{\ell=1}^{n/2}\alpha_\ell\ \overline{\phi}^{(2\ell-1)\ \zeta^x},\quad \overline{\phi}^{n\text{th}\ \zeta^\theta}=\sum_{\ell=1}^{n/2}\alpha_\ell\ \overline{\phi}^{(2\ell-1)\ \zeta^\theta}. \tag{70}$$

The divergence form of the convection term is locally conservative and the energy is conserved, provided that the discrete continuity equation, Eq. (62), is satisfied. Corresponding convection schemes with advective and skew-symmetric forms can also be defined. Analogously to the second order case, the advective and skew-symmetric forms conserve momentum and energy, provided that the discrete continuity equation is satisfied. The replacement of $\overline{J}^{1\zeta^x}$ and $\overline{J}^{1\zeta^\theta}$ by $\overline{J}^{n\text{th}\zeta^x}$ and $\overline{J}^{n\text{th}\zeta^\theta}$ in the denominators improves formal spatial accuracy slightly for non-uniform grids, but is not essential. The introduction of the mixed high and second order method is aimed at improving the modified wave numbers in the stream and azimuthal directions.

5. Pole treatment

5.1. Existing pole treatments with central interpolation

In direct numerical simulations of turbulent pipe flow, Eggels et al. [6] and Akselvoll and Moin [7] introduced the following pole treatment:

$$u_r(x,0,\theta_{k+1/2}) = \widehat{u}_r(x,0,\theta_{k+1/2}), \tag{71}$$

where

$$\widehat{u}_r(x,0,\theta_{k+1/2}) = \frac{u_r(x,r_1,\theta_{k+1/2}) - u_r(x,r_1,\theta_{k+1/2}+\pi)}{2}. \tag{72}$$

The velocity arrangement around the pole is shown in Fig. 4. The above treatment satisfies the antisymmetric relation

$$u_r(x,0,\theta_{k+1/2}) = -u_r(x,0,\theta_{k+1/2}+\pi). \tag{73}$$

However, the corresponding velocity components in Cartesian coordinates are multi-valued ar $r = 0$. Griffin et al. [10] introduced a single-valued representation of the velocity component at $r = 0$. The transformation relations for the vector components between r–θ and y–z planes are Eqs. (30), (31), and

$$u_y = u_r\cos\theta - u_\theta\sin\theta, \tag{74}$$

$$u_z = u_r\sin\theta + u_\theta\cos\theta. \tag{75}$$

Griffin et al. used Eq. (30) to determine u_r at $r = 0$ as

$$u_r(x,0,\theta_{k+1/2}) = \overline{u_y}(x)\cos\theta_{k+1/2} + \overline{u_z}(x)\sin\theta_{k+1/2}. \tag{76}$$

The coefficients, $\overline{u_y}(x)$ and $\overline{u_z}(x)$, are the averaged values of u_y and u_z at $r = 0$ for a given x (on a r–θ plane).

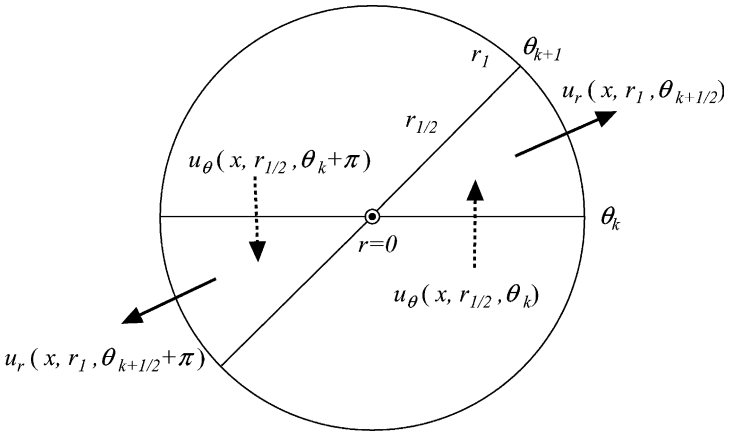

Fig. 4. Velocity arrangement around the pole.

$$\overline{u_y}(x) = \frac{1}{N_\theta}\sum_{k=0}^{N_\theta-1}\left[\widehat{u}_r(x,0,\theta_{k+1/2})\cos\theta_{k+1/2} - \widehat{u}_\theta(x,0,\theta_k)\sin\theta_k\right],$$
$$\overline{u_z}(x) = \frac{1}{N_\theta}\sum_{k=0}^{N_\theta-1}\left[\widehat{u}_r(x,0,\theta_{k+1/2})\sin\theta_{k+1/2} + \widehat{u}_\theta(x,0,\theta_k)\cos\theta_k\right], \tag{77}$$

where $\widehat{u}_r(x,0,\theta_{k+1/2})$ is given by Eq. (72) and $\widehat{u}_\theta(x,0,\theta_k)$ is given by

$$\widehat{u}_\theta(x,0,\theta_k) = \frac{u_\theta(x,r_{1/2},\theta_k) - u_\theta(x,r_{1/2},\theta_k+\pi)}{2}. \tag{78}$$

Griffin et al. introduced one-sided interpolated values instead of $\widehat{u}_r$ and $\widehat{u}_\theta$ in their original paper [10]. Recently, Fukagata and Kasagi [9] introduced a single-valued representation of u_r at $r = 0$ based on the series expansion of Constantinescu and Lele [13]. Their pole treatment can be interpreted as Eq. (76) with

$$\overline{u_y}(x) = -\frac{2}{N_\theta}\sum_{k=0}^{N_\theta-1}\widehat{u}_\theta(x,0,\theta_k)\sin\theta_k,$$
$$\overline{u_z}(x) = \frac{2}{N_\theta}\sum_{k=0}^{N_\theta-1}\widehat{u}_\theta(x,0,\theta_k)\cos\theta_k. \tag{79}$$

The combinations of coefficients, $\overline{u_y}(x)$ and $\overline{u_z}(x)$, are also derived by using least square minimization of the error of Eqs. (30) and (31). The coefficients of Griffin et al. [10] are obtained by least square minimization of Eqs. (30) and (31), i.e. by minimizing the following L^2-error:

$$Q^{r\theta}(x) = \frac{1}{N_\theta}\sum_{k=0}^{N_\theta-1}\left[\ \widehat{u}_r(x,0,\theta_{k+1/2}) - \overline{u_y}(x)\cos\theta_{k+1/2} - \overline{u_z}(x)\sin\theta_{k+1/2}\ \right]^2$$
$$+\frac{1}{N_\theta}\sum_{k=0}^{N_\theta-1}\left[\ \widehat{u}_\theta(x,0,\theta_k) + \overline{u_y}(x)\cos\theta_k - \overline{u_z}(x)\cos\theta_k\ \right]^2. \tag{80}$$

Orthogonality relations of the trigonometric functions are used in the derivation process. The coefficients of Fukagata and Kasagi [9] are derived by least square minimization of Eq. (31), i.e. by minimizing the following L^2-error:

$$Q^{\theta}(x) = \frac{1}{N_\theta}\sum_{k=0}^{N_\theta-1}\left[\ \widehat{u}_\theta(x,0,\theta_k) + \overline{u_y}(x)\cos\theta_k - \overline{u_z}(x)\cos\theta_k\ \right]^2. \tag{81}$$

There exists another coefficient representation, which minimizes the square error of Eq. (30), Q^r:

$$Q^{r}(x) = \frac{1}{N_\theta}\sum_{k=0}^{N_\theta-1}\left[\widehat{u}_r(x,0,\theta_{k+1/2}) - \overline{u_y}(x)\cos\theta_{k+1/2} - \overline{u_z}(x)\sin\theta_{k+1/2}\right]^2. \tag{82}$$

Corresponding coefficients are:

$$\overline{u_y}(x) = \frac{2}{N_\theta}\sum_{k=0}^{N_\theta-1}\widehat{u}_r(x,0,\theta_{k+1/2})\cos\theta_{k+1/2},$$
$$\overline{u_z}(x) = \frac{2}{N_\theta}\sum_{k=0}^{N_\theta-1}\widehat{u}_r(x,0,\theta_{k+1/2})\sin\theta_{k+1/2}. \tag{83}$$

In this study, the multi-valued pole treatment of Eq. (71) is called $M(u_r)$. The single-valued pole treatment of Eq. (76) with Eqs. (77), (79) and (83) are referred to as $S(u_r, u_\theta)$, $S(u_\theta)$ and $S(u_r)$, respectively. The single-valued property is a good indicator for specifying the radial velocity at the pole. However the interpolated values, $\widehat{u}_r$ and $\widehat{u}_\theta$, are not governed by the momentum equation at the pole.

5.2. A new pole treatment

We believe that the best way to obtain u_r at the pole is to solve a discrete radial momentum equation, which is discretized in the same manner as those for the neighboring u_r points. Eq. (12) (and its original form, Eq. (3)) is mathematically singular at $r = 0$. However, the origin of the singularity is not physical but geometrical (coordinate system dependent), as was explained in Section 3. In this study, we propose to introduce the following discrete radial momentum equation that corresponds to Eq. (40) at $r = 0$:

$$\frac{\partial\, u_r}{\partial\, t} + (\text{Conv.-2})_r + \frac{1}{\rho}\frac{1}{h_r}\frac{\delta_2\ \overline{p}^{1\zeta^r}}{\delta_2\ \zeta^r} = \frac{1}{h_x}\frac{\delta_1\ \tau_{xr}}{\delta_1\ \zeta^x} + \frac{1}{h_r}\frac{\delta_1\ \tau_{rr}}{\delta_1\ \zeta^r} + \frac{1}{h_r}\frac{\delta_2}{\delta_2\ \zeta^r}\left(\frac{\Delta\zeta^\theta}{\Delta\theta}\frac{\delta_1\ \tau_{\theta r}}{\delta_1\ \zeta^\theta}\right) + \frac{1}{h_r}\frac{\delta_1}{\delta_1\ \zeta^r}(\tau_{rr} - \tau_{\theta\theta}) + f_r \quad \text{at } r = 0, \tag{84}$$

where $(\text{Conv.-2})_r$ is a generic form and specific forms are defined in Section 4.1. The energy conservative convection schemes can also be applied for the radial momentum equation at the pole. The energy conservation property of the convection term in the region including the pole is confirmed in the same way as that in Section 4.1 with the energy norm of Eq. (56). The introduction of the averaged Jacobian appearing in the denominator of the discrete equation is necessary for removing the singularity. In the case of a uniform grid, the difference between

$$\sum_{i=0}^{N_x-1}\sum_{k=0}^{N_\theta/2-1}\overline{J}^{1\zeta^r}\Big|_{x_{i+1/2},0,\theta_{k+1/2}} + \sum_{i=0}^{N_x-1}\sum_{j=1}^{N_r-1}\sum_{k=0}^{N_\theta-1}\overline{J}^{1\zeta^r}\Big|_{x_{i+1/2},r_j,\theta_{k+1/2}} = \pi r_{N_r-1/2}^2 L_x \tag{85}$$

and

$$\sum_{i=0}^{N_x-1}\sum_{k=0}^{N_\theta/2-1} J|_{x_{i+1/2},0,\theta_{k+1/2}} + \sum_{i=0}^{N_x-1}\sum_{j=1}^{N_r-1}\sum_{k=0}^{N_\theta-1} J|_{x_{i+1/2},r_j,\theta_{k+1/2}} = \pi(r_{N_r-1/2}^2 - r_{1/2}^2)L_x \tag{86}$$

justifies the proposed Jacobian treatment, so the control volume for u_r with $\overline{J}^{1\zeta^r}$ fills a whole domain including the pole, while the standard treatment introduces a hole at the pole because $J|_{x,0,\theta} = 0$. This also reveals that the scheme with denominator J works for simulations in the region excluding $r = 0$ as mentioned at the end of Section 4.1. Note that the Jacobian appearing as a numerator in the convection term of Eq. (84) is standard, i.e. zero at $r = 0$. This condition is required for the energy conservation when the discrete continuity equation is solved with $((J/h_r)u_r) = 0$ at $r = 0$. In addition, the application of $(\text{Pres.-2})_r$ at the pole yields $\partial p/\partial r = 0$, which is not acceptable, while it offers the complete energy conservation for flows including the pole. The reason for selection of the discrete pressure term (the third term on the left hand side of Eq. (84)) at the pole will be explained in Section 6.

Some discrete variables at $r \leqslant 0$ are required for Eq. (84). First of all, we suppose

$$u_x(x, -r, \theta) = u_x(x, r, \theta + \pi), \tag{87}$$

$$u_r(x, -r, \theta) = -u_r(x, r, \theta + \pi), \tag{88}$$

$$J(x,-r,\theta) = J(x,r,\theta+\pi), \tag{89}$$

$$\left(\frac{J}{h_r}u_r\right)\Big|_{x,0,\theta} = 0. \tag{90}$$

Other discrete variables at $r \leqslant 0$ are decided by imposing the condition that Eq. (84) at $(x_{i+1/2}, 0, \theta_{k+1/2})$ is equal to −Eq. (84) at $(x_{i+1/2}, 0, \theta_{k+1/2}+\pi)$, which guarantees the condition of Eq. (88) at $r = 0$. For instance, from the relation,

$$\frac{\delta_1}{\delta_1\ \zeta^r}\left[\overline{\left(\frac{J}{h_r}u_r\right)}^{1\ \zeta^r}\ \overline{u_r}^{1\ \zeta^j}\right]\Big|_{x,0,\theta} = -\frac{\delta_1}{\delta_1\ \zeta^r}\left[\overline{\left(\frac{J}{h_r}u_r\right)}^{1\ \zeta^r}\ \overline{u_r}^{1\ \zeta^j}\right]\Big|_{x,0,\theta+\pi}$$

we get

$$\left(\frac{J}{h_r}u_r\right)\Big|_{x,-r,\theta} = -\left(\frac{J}{h_r}u_r\right)\Big|_{x,r,\theta+\pi}. \tag{91}$$

In the same manner, the following relations are specified for the inviscid terms:

$$\left(\frac{J}{h_x}u_x\right)\Big|_{x,-r,\theta} = \left(\frac{J}{h_x}u_x\right)\Big|_{x,r,\theta+\pi}, \tag{92}$$

$$\left(\frac{J}{h_\theta}u_\theta\right)\Big|_{x,-r,\theta} = \left(\frac{J}{h_\theta}u_\theta\right)\Big|_{x,r,\theta+\pi}, \tag{93}$$

$$\left(\frac{J}{r}\overline{u_\theta}^{1\zeta^\theta}\overline{u_\theta}^{1\zeta^\theta}\right)\Big|_{x,-r,\theta} = -\left(\frac{J}{r}\overline{u_\theta}^{1\zeta^\theta}\overline{u_\theta}^{1\zeta^\theta}\right)\Big|_{x,r,\theta+\pi}. \tag{94}$$

The discrete pressure term satisfies the asymmetric condition. Required relations for the viscous terms are:

$$\tau_{xr}|_{x,0,\theta} = -\tau_{xr}|_{x,0,\theta+\pi}, \tag{95}$$

$$\tau_{rr}|_{x,-r,\theta} = \tau_{rr}|_{x,r,\theta+\pi}, \tag{96}$$

$$\left(\frac{\Delta\zeta^\theta}{\Delta\theta}\frac{\delta_1\ \tau_{\theta r}}{\delta_1\ \zeta^\theta}\right)\Big|_{x,-r,\theta} = \left(\frac{\Delta\zeta^\theta}{\Delta\theta}\frac{\delta_1\ \tau_{\theta r}}{\delta_1\ \zeta^\theta}\right)\Big|_{x,r,\theta+\pi}, \tag{97}$$

$$(\tau_{rr}-\tau_{\theta\theta})|_{x,-r,\theta} = (\tau_{rr}-\tau_{\theta\theta})|_{x,r,\theta+\pi}. \tag{98}$$

Supplementary explanations may be required for the treatment of viscous terms. The radial derivative of u_x in τ_{xr} at the pole is estimated by $(h_r)_{r=0} = 2r_{1/2}$ with $\Delta\zeta^r = 1$ and Eq. (87), so that Eq. (95) is satisfied. Eq. (96) is satisfied with $(h_r)_{r=r_{1/2}} = (h_r)_{r=r_{-1/2}} = r_1$, $\Delta\zeta^r = 1$, and Eq. (88). Eqs. (97), (98) and the corresponding discrete term in Eq. (84) are consistent with Eq. (36) in the sense of second order central finite difference method.

In the staggered grid configuration, we should estimate $\partial\tau_{r\theta}/\partial r$ in the discrete u_θ equation at $r = r_{1/2}$, and therefore we need $\tau_{r\theta}$ at $r = 0$ for the standard central discretization. We introduce a discrete form of Eq. (37) for $\tau_{\theta r}$ at $r = 0$

$$\tau_{\theta r} = \nu \frac{\Delta\zeta^{\theta}}{\Delta\theta} \frac{\delta_1}{\delta_1 \zeta^{\theta}} \left(\frac{1}{h_r} \frac{\delta_2 u_r}{\delta_2 \zeta^{r}} \right) \quad \text{at } r = 0. \tag{99}$$

This discrete form with Eq. (88) satisfies $\tau_{\theta r}|_{x,0,\theta} = \tau_{\theta r}|_{x,0,\theta+\pi}$, which follows from Eq. (34).

Now we can close and solve the discrete system for the flow region including the pole in cylindrical coordinates. However, the velocity components in Cartesian coordinates at $r = 0$, corresponding to u_r obtained from Eq. (84), are still multi-valued. Therefore, the single-valued reconstruction by Eq. (76) with

$$\begin{aligned} \overline{u_y}(x) &= \frac{2}{N_\theta} \sum_{k=0}^{N_\theta - 1} u_r^*(x, 0, \theta_{k+1/2}) \cos\theta_{k+1/2}, \\ \overline{u_z}(x) &= \frac{2}{N_\theta} \sum_{k=0}^{N_\theta - 1} u_r^*(x, 0, \theta_{k+1/2}) \sin\theta_{k+1/2} \end{aligned} \tag{100}$$

is introduced. Here, $u_r^*(x, 0, \theta_{k+1/2})$ is the radial velocity at $r = 0$ obtained from Eq. (84).

In the present pole treatment, the radial velocity at the pole is obtained based on the radial momentum equation with the energy-conservative convection scheme. The single-valued property is satisfied through the single-valued reconstruction at the pole.

6. Numerical tests

6.1. Numerical method

The coupling algorithm of the discrete momentum and continuity equations for the viscous flow is based on the second order splitting method by Dukowicz and Dvinsky [14]. The resulting discrete Poisson equation for the pressure is solved directly using FFT in the periodic directions and tri-diagonal matrix algorithm (TDMA) in the radial direction. Therefore, the discrete continuity equation is satisfied completely except for the round-off error of the computer. The temporal integration scheme is a combined RK3/CN scheme. For the temporal integration scheme the device proposed by Akselvoll and Moin [15] is introduced, where the computational domain is divided into two regions in which terms with derivatives in only one coordinate direction are treated implicitly with the Crank–Nicolson scheme. In this study, second order derivatives in the azimuthal direction are treated implicitly in $0 \leqslant r < r_{N_r/2}$, while second order derivatives in the radial direction are treated implicitly in $r_{N_r/2} \leqslant r \leqslant r_{N_r}$. For the inviscid flow simulations the algorithm is adopted with $\nu = 0$.

6.2. Inviscid flow in a concentric annular pipe

The objective of the first numerical test is to study the energy conservation property of the proposed finite difference scheme. The test flow field is a concentric annular pipe with $R_1/R_2 = 0.1$ and $R_2 - R_1 = D = 1.0$, where R_1 and R_2 are inner and outer radii as shown in Fig. 5. The computational domain is $0 \leqslant x \leqslant L_x (= 4\pi D)$, $R_1 \leqslant r \leqslant R_2$ and $0 \leqslant \theta \leqslant 2\pi$, where the streamwise and azimuthal directions are periodic. The grid resolution, $N_x \times N_r \times N_\theta$, is $16 \times 16 \times 32$. The radial grid distribution is non-uniform with a hyperbolic-tangent type stretching function, while the grid spacings in the periodic directions are uniform. The initial condition of the simulation is a flow field computed by a viscous simulation with $\nu = 1/360$ and $f_x = -2$. The inviscid simulations are performed with $\nu = f_x = f_r = f_\theta = 0$. The time increment, Δt, is 0.00005. Fig. 6 shows the evolution of total kinetic energy for the inviscid flow simulation. The total kinetic energy is defined as

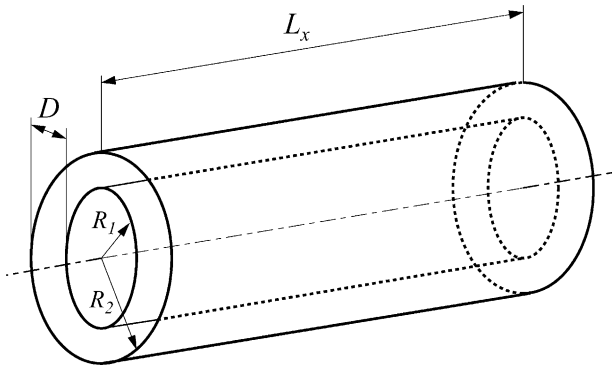

Fig. 5. Concentric annular flow.

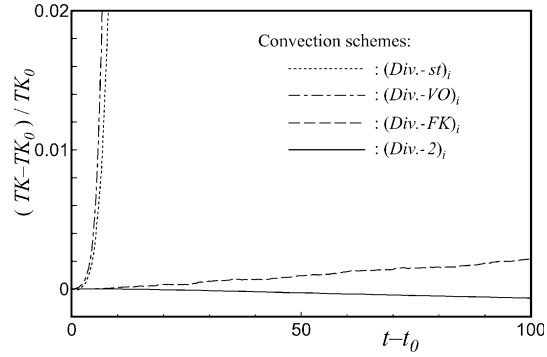

Fig. 6. Total kinetic energy evolution for inviscid flow in a concentric annular pipe.

$$TK = \frac{1}{2}\sum_{i=0}^{N_x-1}\sum_{j=0}^{N_r-1}\sum_{k=0}^{N_\theta-1}\left[\overline{J^{1\zeta^x}}^{1\zeta^x}u_x u_x + \overline{J^{1\zeta^r}}^{1\zeta^r}u_r u_r + \overline{J^{1\zeta^\theta}}^{1\zeta^\theta}u_\theta u_\theta\right]_{x_{i+1/2},r_{j+1/2},\theta_{k+1/2}},$$

where $(x_{i+1/2}, r_{j+1/2}, \theta_{k+1/2})$ corresponds to the pressure node, and $r_0 = R_1$ and $r_{N_r} = R_2$. The initial value is $TK_0 = 13308.1725$ at $t = t_0$. Numerical simulations were performed for a number of existing finite difference schemes in cylindrical coordinates. The details of these schemes are given in Appendix B. The inviscid simulations with the standard, $(\text{Div.-st})_i$, and Verzicco and Orlandi, $(\text{Div.-VO})_i$, type convection schemes diverge soon, while the total kinetic energy with a Fukagata and Kasagi type convection scheme, $(\text{Div.-FK})_i$, gradually increases with time. This coincides with the results reported in [9]. As it is clearly seen in the figure, the total kinetic energy of the proposed scheme, $(\text{Div.-2})_i$, slightly decreases with time. Fig. 7 shows the time increment dependence of the error with the present scheme at $t - t_0 = 100$. The error slope of $(\text{Div.-2})_i$ is Δt^3, which is the error due to the time integration scheme. Therefore, the present finite difference scheme itself conserves the kinetic energy completely with the exception of the temporal integration error.

6.3. Inviscid flow in a straight pipe

The second numerical test is designed to check the energy conservative property of the present pole treatment. The test flow field is a straight pipe flow with radius $R(= 1.0)$ as shown in Fig. 8. The

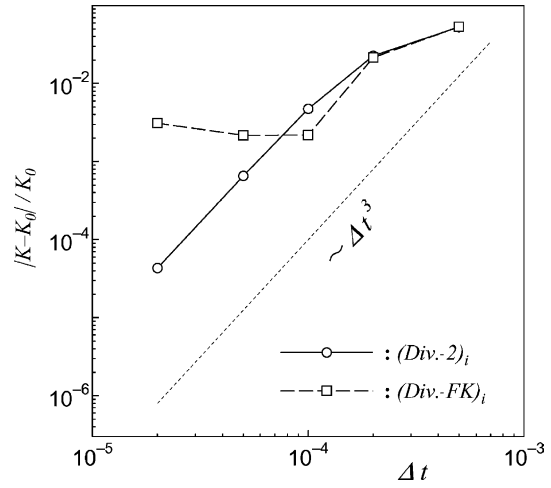

Fig. 7. Dependence of the total kinetic energy error on time increment for (Div.-2) and (Div.-FK).

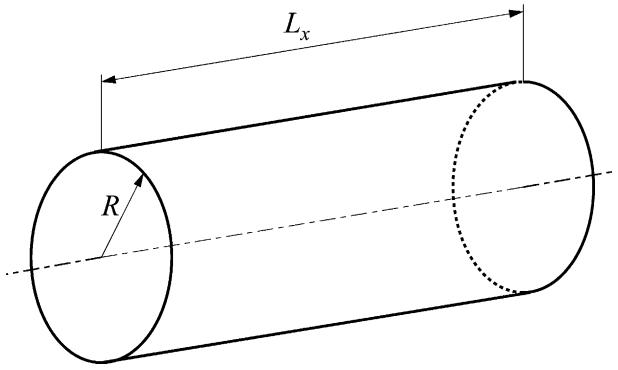

Fig. 8. Straight pipe flow.

computational domain is $0 \leqslant x \leqslant L_x (= 4\pi R)$, $0 \leqslant r \leqslant R$ and $0 \leqslant \theta \leqslant 2\pi$, where the streamwise and azimuthal directions are periodic. The grid resolution, $N_x \times N_r \times N_\theta$, is $16 \times 16 \times 32$. The radial grid distribution is also non-uniform with a hyperbolic-tangent type stretching function, while the grid spacings in the periodic directions are uniform. The initial condition of the simulation is a flow field computed by a viscous simulation with $\nu = 1/180$, $f_x = -2$ and $f_r = f_\theta = 0$. The inviscid simulations are done with $\nu = f_x = f_r = f_\theta = 0$. The time increment, Δt, is 0.001. The difference of the total kinetic energy evolution by different pole treatments is illustrated in Fig. 9. The total kinetic energy is defined as in the previous test case except that $r_0 = 0$ and $r_{N_r} = R$. The initial value is $TK_0 = 4804.65355$ at $t = t_0$. The finite difference scheme except at $r = 0$ is the present one with $(\text{Div.-2})_i$. The energy with the multi-valued pole treatment ($M(u_r)$) diverges quickly. The energy with the single-valued pole treatments ($S(u_r, u_\theta)$, $S(u_\theta)$, $S(u_r)$) gradually increase and finally diverge, while they are better than the multi-valued treatment. Therefore, previously existing pole treatments inject unphysical kinetic energy production at $r = 0$. One of the main objectives of the present study is to introduce the radial momentum equation to define u_r at $r = 0$. Direct application of the scheme proposed in Section 4.1 at $r = 0$ offers complete kinetic energy conservation (*zero* in Fig. 9). A

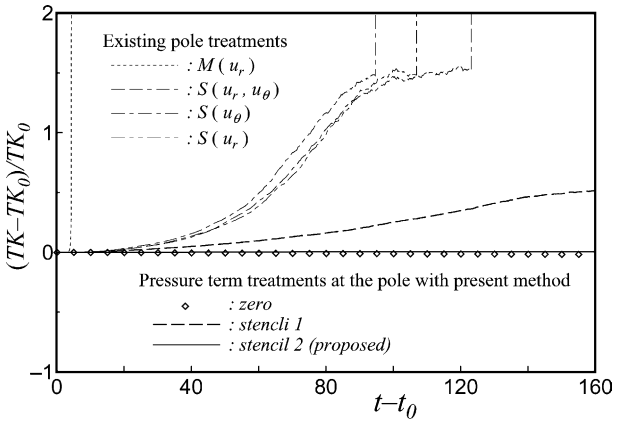

Fig. 9. Kinetic energy evolution for inviscid flow in a straight pipe.

slight decrease comes from the time integration error. However, it yields $\partial p/\partial r = 0$ at $r = 0$, which is not acceptable from the physical point of view. Therefore, we have examined an alternative treatment of the pressure term at the pole. Two possible candidates were the discrete pressure terms with stencil 1 or 2:

$$\frac{\partial p}{\partial r} \sim \frac{1}{h_r}\frac{\delta_1\, p}{\delta_1\, \zeta^r}, \tag{101}$$

$$\frac{\partial p}{\partial r} \sim \frac{1}{h_r}\frac{\delta_2\, \overline{p}^{1\zeta^r}}{\delta_2\, \zeta^r}. \tag{102}$$

The kinetic energy of the case with Eq. (101), *stencil 1* in Fig. 9, gradually increases with time while it is much better than the cases with the existing pole treatments. On the other hand, the case with the discrete pressure term given by Eq. (102), *stencil 2* in Fig. 9, conserves the energy. This is the reason for selecting the discrete pressure term proposed in Section 5.2.

6.4. Large eddy simulation of turbulent pipe flow

The third numerical test is the large eddy simulation (LES) of turbulent pipe flow. The computational domain is $0 \leqslant x \leqslant L_x (= 4\pi R)$, $0 \leqslant r \leqslant R$ and $0 \leqslant \theta \leqslant 2\pi$, where the streamwise and azimuthal directions are periodic. The grid resolution, $N_x \times N_r \times N_\theta$, is $16 \times 64 \times 16$ and $48 \times 64 \times 48$. The radial grid distribution is also non-uniform with a hyperbolic-tangent type stretching function, while the grid spacings in the periodic directions are uniform. The numerical parameters are $\nu = 1/180$, $R = 1$, $f_x = -2$, and $f_r = f_\theta = 0$. The corresponding Reynolds number is 180 based on the friction velocity, u_τ, and the pipe radius, R. The subgrid scale model is the dynamic Smagorinsky model of Germano et al. [16] with the least square modification of Lilly [17]. For detailed implementation of the model please refer to Morinishi and Vasilyev [18,19], where the model is compared with other subgrid scale models in plane channel flow. Here we just use it for cylindrical coordinates. Figs. 10 and 11 show the computational results for $16 \times 64 \times 16$ and $48 \times 64 \times 48$ grids, respectively. The results with the respective mixed high and second order schemes are labelled as 4th, 8th and 12th FDM. The symbols (○) indicate the direct numerical simulation (DNS) data of pipe flow by Fukagata and Kasagi [9] with $256 \times 96 \times 128$ grids for $L_x = 10R$ at $Re_\tau = 180$. The LES with the 8th and higher order simulations maintain the turbulent flow even for $16 \times 64 \times 16$ grids, while the flow

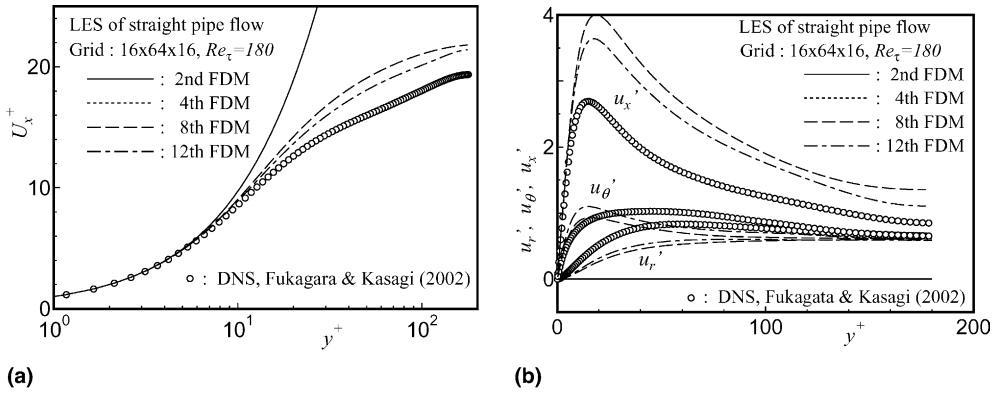

Fig. 10. LES of turbulent pipe flow at $Re_\tau = 180$ with $16 \times 64 \times 16$ grid: (a) mean velocity profiles; (b) turbulence intensities.

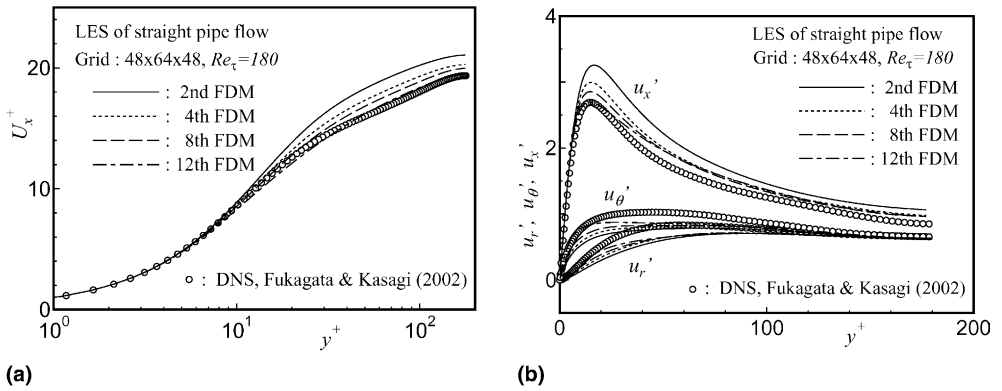

Fig. 11. LES of turbulent pipe flow at $Re_\tau = 180$ with $48 \times 64 \times 48$ grid: (a) mean velocity profiles; (b) turbulence intensities.

with the second and fourth order schemes are laminarized. This implies a possibility that an LES of pipe flow with a more sophisticated subgrid scale model offers reliable results with the high order scheme even for the coarse grid. In addition, the isotropy in the r–θ plane ($u_r' = u_\theta'$) is recovered close to the pole. The LES with the second order simulation maintains the turbulent flow with a $48 \times 64 \times 48$ grid. However, the reliability of the mean velocity and turbulence intensities profiles are not enough. Considering the grid configuration for the pipe, increasing the order of accuracy only in the periodic directions is a recommended device for LES. The high order schemes offer better results than the second order scheme. The factors of computational cost of the simulation per time step with $16 \times 64 \times 16$ grid for the 4th, 8th and 12th order schemes to the second one are 1.26, 1.78 and 2.29, respectively. On the other hand, the factors of the second order scheme with $32 \times 64 \times 32$, $48 \times 64 \times 48$ and $64 \times 64 \times 64$ grids to $16 \times 64 \times 16$ grid are 2.08, 3.25 and 4.43, respectively. In addition, the use of finer mesh results in memory increase. Therefore, the mixed high order scheme is recommended for the LES of turbulent pipe flow. The mixed high order schemes should be beneficial for the DNS of pipe flow, although the merit of the schemes was tested only for the LES. The representation of high order statistics with the second order scheme requires higher grid resolution than one for mean velocity and turbulence intensity representation. For instance, the skewness factor of u_r as shown in Fig. 12 is strongly affected by the order of the method.

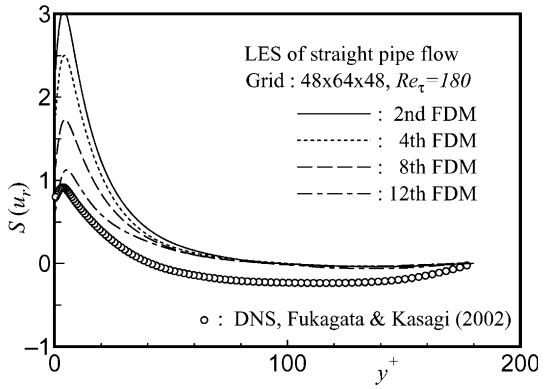

Fig. 12. Skewness factor of u_r for the LES at $Re_\tau = 180$ with $48 \times 64 \times 48$ grid.

7. Conclusions

The main objective of the present study was to improve the numerical simulation of incompressible flow in cylindrical coordinates. A fully conservative finite difference scheme for staggered and non-uniform grids is proposed. The complete conservation is achieved by performing all discrete operations in computational space. This is an appropriate extension of the fully conservative finite difference scheme by Morinishi et al. [2] to non-uniform grids in cylindrical coordinates. A novel pole treatment is also proposed, where the radial momentum equation is solved to determine the velocity at the pole. The singularity is properly removed by analytical and numerical techniques. The single-valued property of the velocity at the pole is satisfied through the proposed reconstruction process. Reliability and conservation properties of the proposed scheme are numerically verified in inviscid flow simulations. The benefits of the proposed mixed high and second order fully conservative scheme for large eddy simulations of turbulent flow in cylindrical coordinates are demonstrated for turbulent pipe flow.

Acknowledgements

The first author (Y. Morinishi) was partially supported by the Center for Promotion of Computational Science and Engineering, Japan Atomic Energy Research Institute, whose support is gratefully acknowledged. Partial support for the second author (O.V. Vasilyev) was provided by the National Science Foundation under Grant Nos. EAR-0242591, EAR-0327269, and ACI-0242457 and National Aeronautics and Space Administration under Grant No. NAG-1-02116.

Appendix A. Discrete operators

The first appendix presents the discrete operators used in this paper. The following discrete operators are basically the same as those proposed in [2] except that the present operations are done in a computational space in cylindrical coordinates.

The interpolation operator with stencil n acting on ϕ in the ζ^x direction is described as

$$\overline{\phi}^{n\,\zeta^x}(\zeta^x,\zeta^r,\zeta^\theta) = \frac{\phi(\zeta^x + n\Delta\zeta^x/2,\zeta^r,\zeta^\theta) + \phi(\zeta^x - n\Delta\zeta^x/2,\zeta^r,\zeta^\theta)}{2}, \tag{A.1}$$

where $\overline{\phi}^{n\,\zeta^r}$ and $\overline{\phi}^{n\,\zeta^\theta}$ are defined in the same manner as $\overline{\phi}^{n\,\zeta^x}$. The finite difference operator with stencil n acting on ϕ in the ζ^x direction is given by

$$\frac{\delta_n\ \phi}{\delta_n\ \zeta^x}(\zeta^x,\zeta^r,\zeta^\theta)=\frac{\phi(\zeta^x+n\Delta\zeta^x/2,\zeta^r,\zeta^\theta)-\phi(\zeta^x-n\Delta\zeta^x/2,\zeta^r,\zeta^\theta)}{n\Delta\zeta^x}, \tag{A.2}$$

where $\delta_n\ \phi/\delta_n\ \zeta^r$ and $\delta_n\ \phi/\delta_n\ \zeta^\theta$ are defined in the same manner as $\delta_n\ \phi/\delta_n\ \zeta^x$. An interpolation operator for the product of ϕ and ψ is described as

$$\begin{aligned}\widetilde{\phi\psi}^{n\,\zeta^x}(\zeta^x,\zeta^r,\zeta^\theta)&=\frac{1}{2}\phi(\zeta^x+n\Delta\zeta^x/2,\zeta^r,\zeta^\theta)\cdot\psi(\zeta^x-n\Delta\zeta^x/2,\zeta^r,\zeta^\theta)\\&\quad+\frac{1}{2}\psi(\zeta^x+n\Delta\zeta^x/2,\zeta^r,\zeta^\theta)\cdot\phi(\zeta^x-n\Delta\zeta^x/2,\zeta^r,\zeta^\theta),\end{aligned} \tag{A.3}$$

where $\widetilde{\phi\psi}^{n\,\zeta^r}$ and $\widetilde{\phi\psi}^{n\,\zeta^\theta}$ are defined in the same manner as $\widetilde{\phi\psi}^{n\,\zeta^x}$. Note that $n\zeta^j$, appearing as a superscript, does not follow the summation convention.

Following are useful identities associated with the discrete operators:

$$\frac{\delta_n\ \overline{\phi}^{m\,\zeta^i}}{\delta_n\ \zeta^j}=\overline{\frac{\delta_n\ \phi}{\delta_n\ \zeta^j}}^{m\,\zeta^i},\quad \frac{\delta_n\ \overline{\phi}^{m\,t}}{\delta_n\ \zeta^j}=\overline{\frac{\delta_n\ \phi}{\delta_n\ \zeta^j}}^{m\,t}, \tag{A.4}$$

$$\frac{\delta_n\ \psi\cdot\overline{\phi}^{n\,\zeta^j}}{\delta_n\ \zeta^j}=\overline{\psi\ \frac{\delta_n\ \phi}{\delta_n\ \zeta^j}}^{n\,\zeta^j}+\phi\ \frac{\delta_n\ \psi}{\delta_n\ \zeta^j} \tag{A.5}$$

$$\phi\ \frac{\delta_n\ \psi\cdot\overline{\phi}^{n\,\zeta^j}}{\delta_n\ \zeta^j}=\frac{1}{2}\ \frac{\delta_n\ \psi\cdot\widetilde{\phi\phi}^{n\,\zeta^j}}{\delta_n\ \zeta^j}+\frac{1}{2}\ \phi\phi\ \frac{\delta_n\ \psi}{\delta_n\ \zeta^j} \tag{A.6}$$

In this study, we set $\Delta\zeta^x=\Delta\zeta^r=\Delta\zeta^\theta=1$ in the computational space.

We now define two concepts of discrete conservation. We say that a discretization of a term, $Q=(1/J)(\partial\phi/\partial\zeta^j)$, is *locally* conservative if it can be written in the following from:

$$Q=\sum_n\frac{1}{J}\frac{\delta_n(\Phi^n)}{\delta_n\zeta^j}. \tag{A.7}$$

We say that a discretization of a term, Q, is *globally* conservative if the following relation holds in a periodic field:

$$\sum_{\zeta^x}\sum_{\zeta^r}\sum_{\zeta^\theta}\ Q\ \Delta V=0, \tag{A.8}$$

where $\Delta V=J\prod_{j=1}^{3}\Delta\zeta^j$. Note that in the periodic case the local conservation (A.7) implies global conservation. Also note that the definition (A.8) is a discrete analogue of Eq. (24). Finally, the following summation property is used in the proof of the global energy conservation in Section 4.1, Eqs. (59) and (60), for the non-conservative terms in the periodic or zero-bounded directions.

$$\sum_{i=1/2}^{N_j-1/2}\overline{\psi\ \overline{\phi}^{1\zeta^j}}^{\zeta^j}=\sum_{i=1/2}^{N_j-1/2}\overline{\psi}^{1\zeta^j}\phi. \tag{A.9}$$

Appendix B. Existing convection schemes for cylindrical coordinates

To indicate the difference between the proposed and existing schemes, typical staggered finite difference schemes in a cylindrical coordinate system are interpreted and represented in the form of Eqs. (47)–(49). Therefore, the following schemes have the essence of the original formulation, while they are not identical to the original ones for the case of a non-uniform grid. In addition, the following schemes have better conservation properties than the original formulations.

Standard type [6,7]:

$$(\text{Div.-st})_x = \frac{1}{\overline{J}^{1\zeta^x}} \frac{\delta_1}{\delta_1\ \zeta^j}\left[\frac{J}{h_j}\ \overline{u_j}^{1\zeta^x}\overline{u_x}^{1\zeta^j}\right], \tag{B.1}$$

$$(\text{Div.-st})_r = \frac{1}{\overline{J}^{1\zeta^r}} \frac{\delta_1}{\delta_1\ \zeta^j}\left[\frac{J}{h_j}\ \overline{u_j}^{1\ \zeta^r}\overline{u_r}^{1\ \zeta^j}\right] - \frac{1}{r}\ \overline{\overline{u_\theta}^{1\zeta^\theta}}^{1\zeta^r}\overline{\overline{u_\theta}^{1\zeta^\theta}}^{1\zeta^r} \tag{B.2}$$

$$(\text{Div.-st})_\theta = \frac{1}{\overline{J}^{1\zeta^\theta}} \frac{\delta_1}{\delta_1\ \zeta^j}\left[\frac{J}{h_j}\overline{u_j}^{1\ \zeta^\theta}\overline{u_\theta}^{1\ \zeta^j}\right] + \frac{1}{r}\ u_\theta\ \overline{\overline{u_r}^{1\zeta^r}}^{1\ \zeta^\theta} \tag{B.3}$$

Verzicco and Orlandi type [8]: To remove the pole singularity, Verzicco and Orlandi [8] introduced the quantity ru_r. Here we interpret it as $q_j = Ju_j$. Rewriting the radial convective term of Eq. (48) in terms of q_j we obtain

$$\frac{1}{\overline{J}^{1\zeta^r}} \frac{\delta_1}{\delta_1\ \zeta^j}\left[\overline{\left(\frac{q_j}{h_j}\right)}^{1\ \zeta^r}\overline{\left(\frac{q_r}{J}\right)}^{1\ \zeta^j}\right] - \frac{1}{\overline{J}^{1\zeta^r}}\ \overline{\left[\frac{J}{r}\ \overline{\left(\frac{q_\theta}{J}\right)}^{1\zeta^\theta}\overline{\left(\frac{q_\theta}{J}\right)}^{1\zeta^\theta}\right]}^{1\ \zeta^r}.$$

The first term is still singular when the discrete equation is adopted at the u_r node adjacent to the singular point. Therefore, they replaced it as

$$\frac{1}{\overline{J}^{1\zeta^r}} \frac{\delta_1}{\delta_1\ \zeta^j}\left[\overline{\left(\frac{q_j}{h_j}\right)}^{1\ \zeta^r}\ \frac{1}{J}\ \overline{q_r}^{1\ \zeta^j}\right] - \frac{1}{\overline{J}^{1\zeta^r}}\ \overline{\left[\frac{J}{r}\ \overline{\left(\frac{q_\theta}{J}\right)}^{1\zeta^\theta}\overline{\left(\frac{q_\theta}{J}\right)}^{1\zeta^\theta}\right]}^{1\ \zeta^r}.$$

This is equivalent to the following form:

$$(\text{Div.-VO})_r = \frac{1}{\overline{J}^{1\zeta^r}} \frac{\delta_1}{\delta_1\ \zeta^j}\left[\overline{\left(\frac{J}{h_j}u_j\right)}^{1\ \zeta^r}\ \frac{1}{J}\ \overline{(Ju_r)}^{1\ \zeta^j}\right] - \frac{1}{\overline{J}^{1\zeta^r}}\ \overline{\left(\frac{J}{r}\overline{u_\theta}^{1\zeta^\theta}\overline{u_\theta}^{1\zeta^\theta}\right)}^{1\ \zeta^r} \tag{B.4}$$

We call this scheme as Verzicco and Orlandi type. It is apparent that the energy conservation property is destroyed at the replacement stage, since this scheme does not require u_r at the pole.

Fukagata and Kasagi type [9]: The convective scheme by Fukagata and Kasagi [9] is basically close to our scheme. Apparent differences appear in the radial and azimuthal components.

$$\begin{aligned}(\text{Div.-FK})_r = {} & \frac{1}{\chi}\frac{1}{\overline{J}^{1\zeta^r}} \frac{\delta_1}{\delta_1\ \zeta^x}\left[\overline{\left(\frac{J}{h_x}u_x\right)}^{1\ \zeta^r}\overline{u_r}^{1\ \zeta^x}\right] + \frac{1}{\overline{J}^{1\zeta^r}} \frac{\delta_1}{\delta_1\ \zeta^r}\left[\overline{\left(\frac{J}{h_r}u_r\right)}^{1\ \zeta^r}\overline{u_r}^{1\ \zeta^r}\right] \\ & + \frac{1}{\overline{J}^{1\zeta^r}} \frac{\delta_1}{\delta_1\ \zeta^\theta}\left[\overline{\left(\frac{J}{h_\theta}u_\theta\right)}^{1\ \zeta^r}\overline{u_r}^{1\ \zeta^\theta}\right] - \frac{1}{r}\frac{1}{h_r}\ \overline{\left[h_r\ \overline{(u_\theta u_\theta)}^{1\zeta^\theta}\right]}^{1\ \zeta^r},\end{aligned} \tag{B.5}$$

$$(\text{Div.-FK})_\theta = \frac{1}{\overline{J}^{1\zeta^\theta}} \frac{\delta_1}{\delta_1\ \zeta^j} \left[\overline{\left(\frac{J}{h_j} u_j\right)}^{1\ \zeta^\theta} \overline{u_\theta}^{1\ \zeta^j} \right] + \frac{1}{r}\ u_\theta\ \overline{\overline{u_r}^{1\zeta^r}}^{1\ \zeta^\theta}, \tag{B.6}$$

where the ad hoc coefficient χ appeared in the first term of Eq. (B.5) is defined as $\chi = \overline{(rh_r)}^{1\ \zeta^r}/(rh_r)$. The coefficient χ is unity when the radial grid is uniform, and their finite difference convective scheme is equivalent to ours when the grid is uniform. However, their scheme does not conserve energy for non-uniform meshes, although it is better than the other existing ones and seems not to cause problem for viscous flow simulations. Also the last terms in Eqs. (B.5) and (B.6) conserve energy, while they are different from our formulation. Note that these terms conserve energy globally, even though the authors claimed it as locally conservative.

References

[1] F.H. Harlow, J.E. Welch, Numerical calculation of time-dependent viscous incompressible flow of fluid with free surface, Phys. Fluids 8 (1965) 2182–2189.
[2] Y. Morinishi, T. Lund, O.V. Vasilyev, P. Moin, Fully conservative higher order finite difference schemes for incompressible flow, J. Comput. Phys. 143 (1998) 90–124.
[3] O.V. Vasilyev, High order finite difference schemes on non-uniform meshes with good conservation properties, J. Comput. Phys. 157 (2000) 746–761.
[4] T. Kajishima, Finite-difference method for convective terms using non-uniform grid, Trans. JSME B 65-633 (1999) 1607–1612 (in Japanese).
[5] F. Ham, F.S. Lien, A.B. Strong, A fully conservative second-order finite difference scheme for incompressible flow on nonuniform grids, J. Comput. Phys. 177 (2002) 117–133.
[6] J.G. Eggels, F. Unger, M.H. Weiss, J. Westerweel, R.J. Adrian, R. Friedrich, F.T.M. Nieuwstadt, Fully developed turbulent pipe flow: a comparison between direct numerical simulation and experiment, J. Fluid Mech. 268 (1994) 175–209.
[7] K. Akselvoll, P. Moin, Large eddy simulation of turbulent confined coannular jets and turbulent flow over a backward facing step, Stanford University Report, TF-63, 1995.
[8] R. Verzicco, P. Orlandi, A finite-difference scheme for three-dimensional incompressible flows in cylindrical coordinates, J. Comput. Phys. 123 (1996) 402–414.
[9] K. Fukagata, N. Kasagi, Highly energy-conservative finite difference method for the cylindrical coordinate system, J. Comput. Phys. 181 (2002) 478–498.
[10] M.D. Griffin, E. Jones, J.D. Anderson Jr, A computational fluid dynamics technique valid at the centerline for non-axisymmetric problems in cylindrical coordinates, J. Comput. Phys. 30 (1979) 352–360.
[11] K. Mohseni, T. Colonius, Numerical treatment of polar coordinate singularities, J. Comput. Phys. 151 (2000) 787–795.
[12] M. Vinokur, Conservation equations of gasdynamics in curvilinear coordinate systems, J. Comput. Phys. 14 (1974) 105–125.
[13] G.S. Constantinescu, S. Lele, A new method for accurate treatment of flow equations in cylindrical coordinates using series expansions, CTR Annual Research Briefs 2000, Center for Turbulence Research, NASA Ames and Stanford University Press, Stanford, CA, 2001, pp. 199–210.
[14] J.K. Dukowicz, A.S. Dvinsky, Approximation as a higher order splitting for the implicit incompressible flow equations, J. Comput. Phys. 102 (1992) 334–336.
[15] K. Akselvoll, P. Moin, An efficient method for temporal integration of the Navier–Stokes equations in confined axisymmetric geometries, J. Comput. Phys. 125 (1996) 454–463.
[16] M. Germano, U. Piomelli, P. Moin, W.H. Cabot, A dynamic subrid-scale eddy viscosity model, Phys. Fluids A 3 (1991) 1760–1765.
[17] D.K. Lilly, A proposed modification of the Germano subgrid scale closure method, Phys. Fluids A 4 (1992) 633–635.
[18] Y. Morinishi, O.V. Vasilyev, A recommended modification to the dynamic two-parameter mixed subgrid scale model for large Eddy simulation of wall bounded turbulent flow, Phys. Fluids 13 (2001) 3400–3410.
[19] Y. Morinishi, O.V. Vasilyev, Vector level identity for dynamic subgrid scale modeling in large eddy simulation, Phys. Fluids 14 (2002) 3616–3623.